

Micro-tomography analysis of fusion material samples

EFDA TW4-TTMI-003 D6

May-September 2006

Ion Tiseanu, Teddy Craciunescu, Nicolae-Bogdan Mandache, Florin Gherendi

Task: TW6-TTMI 003

Deliverable D2, 31-12-2006

IFMIF Test Facilities: X-ray microtomography of a full rig and assessment of its applicability for irradiated samples

Introduction

Recently FZ Karlsruhe has refined the HFTM rig design and manufacturing process and is going to fabricate fully equipped and instrumented irradiation rigs (proposed in Deliverable 1). In addition to the NDT task performed on the HFTM prototype in 2005 one would need to identify the NaK filling height and distribution in the specimen volume and, even more challenging, to assess the quality of the brazing material layer. Also, FZK needs a reliable method for the NDT investigation of the heater plates of the flat duct test-section of ITHEX. This subtask will cover these topics as well as other NDT inspections that might be of interest. Another goal of this subtask is to refine the newly proposed methodology for the simulation of the influence of the sample radioactivity on the tomographic reconstruction quality and to propose practical procedures to mitigate its effects.

X-ray microtomography of a full rig

In the year 2005, by extensive experiments we determined that for the currently measured capsule the geometry resolution is about 30-50 microns for characteristic dimension of 50 mm. This resolution can be guaranteed up to sample size of characteristic dimension of 100 mm. Voids of 30 microns diameter and cracks of 30 microns width can be detected. It was concluded that the absolute error of geometrical measurements should be sufficient for the assessment of the structural integrity of the irradiation capsule and for the geometry description of the thermal-hydraulic modelling.

In 2006 further refinements of the tomographic reconstruction techniques were performed in order to obtain improved quality images. A representative result is presented in Fig. 1 which presents the comparison of tomographic reconstruction with the CAD drawing of the rig. One can note the ability of the tomography inspection to precisely localize and identify the miniaturized samples and the instrumentation elements. Figure 2 (see inserts) shows the ability of the tomography inspection method to detect, even quantitatively, the weak heat coupling regions between the heater coil and the capsule wall. Thus, one can clearly see gaps of up to 1 mm between the heater clad and the groove surface. Further tests will be carried out in order to qualify the thermal contact of the heater wires attached to the capsules by brazing them into grooves.

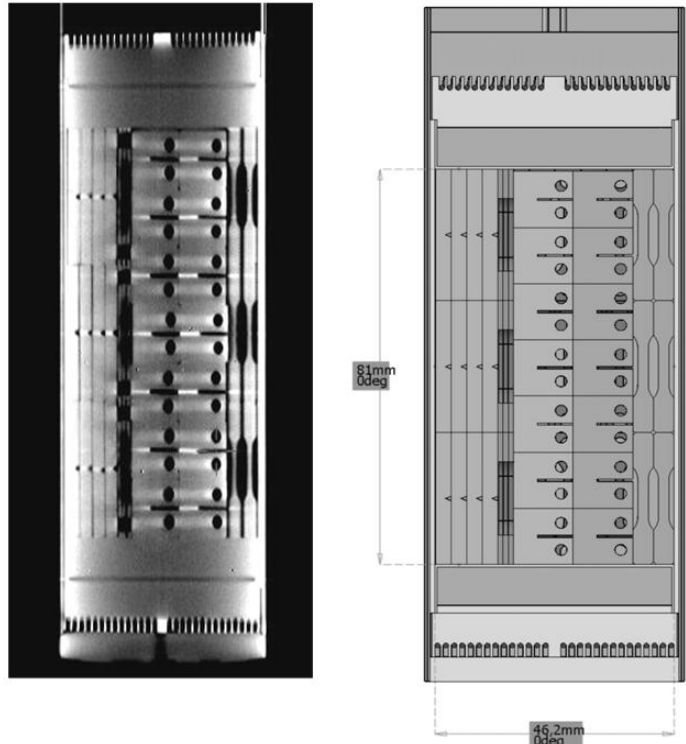


Figure 1 - X-ray microtomography reconstruction and picture of the irradiation capsule, shown as a CAD model on the right.

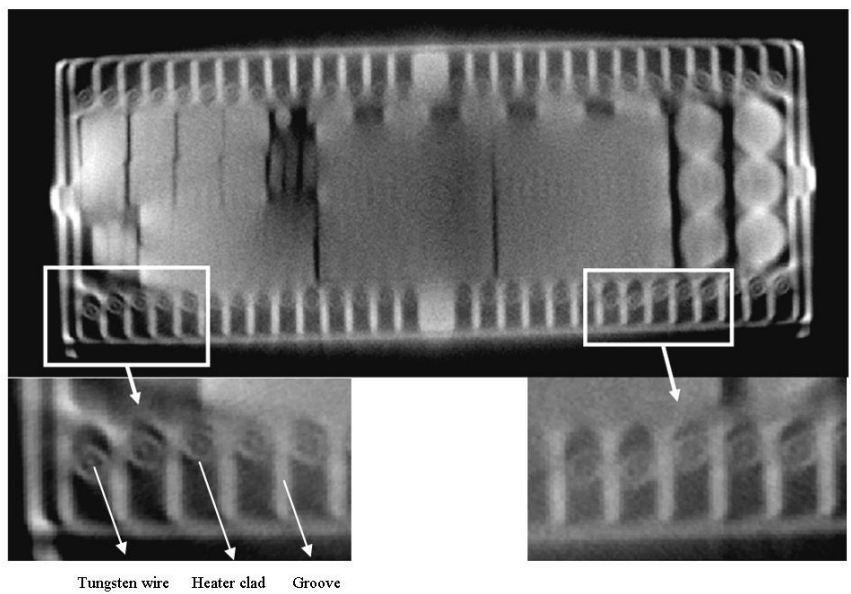


Figure 4 Tomographic cross-section that illustrates the gap (lack of thermal contact) between the heater coil and the groove channel. As dimensional reference one can use the heater diameter of 1 mm.

Assessment of the applicability of X-ray tomography for irradiated samples

The qualification of structural materials in a future fusion reactor requires long-term irradiation in fusion-relevant neutron spectra leading to material damages of up to 150 dpa. IFMIF (International Fusion Materials Irradiation Facility) promises to satisfy the requirements of fusion-relevant material tests regarding the parameters irradiation damage, test volume and neutron flux. Presently, the X-ray micro-tomography is the only reliable solution for official inspections of the structural integrity of IFMIF complete assemblies before, during maintenance (beam-off) periods and after irradiation campaigns. The main challenge to the well established transmission microtomography inspection is the influence of the sample radioactivity (produced by neutron activation) on the tomographic reconstruction quality.

The evaluation of this influence was started in a study performed in 2005, for a miniaturized sample. As far as we know this study was one of the first approaches on this topic. The methodology was fully established, and therefore, in 2006, we continued the study for the specific configuration of newly manufactured IFMIF irradiation capsules also incorporating the latest activation data.

Materials and methods

In computed X-ray transmission tomography the reconstruction is obtained from a number of X-ray radiographies obtained at different rotations of the investigated object. Let I_R be the radiographic image at fixed rotation angle. In the case of a radioactive sample, gamma radiation is emitted from the sample and detected. The image induced by the gamma radiography is called the auto-radiography I_{AR} of the object. The auto-radiography produces a smearing effect superimposed on the on the radiographies (Fig. 5). The effective image formed on the detector is $I_{eff} = I_R + I_{AR}$. This alters of course the X-ray tomographic reconstruction. In order to try to remove the effect induced by the radioactivity of the sample, a supplementary measurement must be performed: the sample is measured in the absence of the X-rays, in the same conditions as in the case when the X-ray tube is on. This enables the acquisition of auto-radiographic images I'_{AR} similar to the auto-radiographies incorporated in I_{eff} . The difference between I_R and I'_{AR} is determined by the noise in the auto-radiographic images. I'_{AR} can be subtracted from I_{eff} in order to obtain $I'_R = I_{eff} - I'_{AR}$, a version of I_R . Of course, $I'_R \neq I_R$. This difference induces residual effects. In consequence, the main steps, for the evaluation of the influence of gamma radioactivity of the sample are the followings:

- measurement of the X-ray radiographies I_R .
- numerical simulation of autoradiography I_{AR} of the investigated object (i.e. the image obtained on the detector due to the gamma emission)
- formation of the effective radiography I_{eff} by combining the radiography I_R and the autoradiography I_{AR} in order to obtain realistic data which in case of a X-ray transmission tomographic analyses performed on an irradiated capsule
- numerical simulation of autoradiography I'_{AR} , which will be subtracted from I_{eff} to obtain I'_R .
- tomographic reconstruction using I'_R , and quality reconstruction analysis.

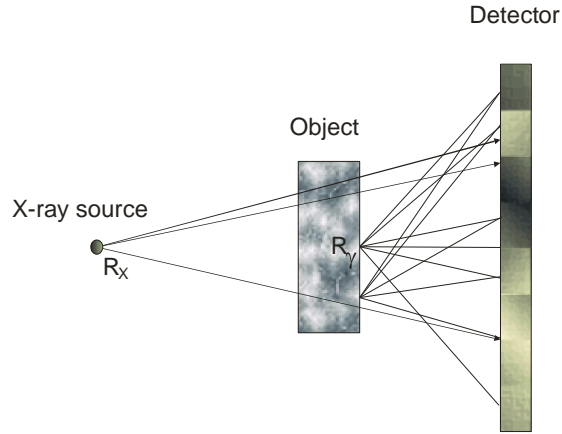


Figure 5 – Radiography and auto-radiography image formation. R_x – X rays emitted in a cone-beam from one point, R_γ - γ rays emitted in a cone-beam from any point of the object. The volume distribution of the gamma emission is responsible for the smearing effect.

Measured radiographies were obtained in a previous work [1-2]. The main parameters describing the tomographic experiment are listed in Table 1.

Table 1.

Source parameters	HV = 215 kV I=650 μ A
Filter	2 mm Cu
Source	VISCOM micro- focus open X-ray tube 225 kV / 300 W
Detector	GOS (Gd_2O_2S) - KODAK Scintillation LANEX screen filter, 409.6 x 409.6 x 0.53 mm, 1024 x 1024 pixels
Sample	HFTM irradiation capsule
Geometry	Source – Object distance: 228 mm Source – Detector distance: 1503 mm Magnification: 6.6 720 equidistant angles

For the numerical simulations, a working environment able to provide a realistic numerical simulation was established on the basis of SIMIND Monte Carlo simulation code [3-4] and on the integrated TIGER series (ITS) time-independent multimaterial and multidimensional-coupled electron/photon Monte Carlo transport code [5].

SIMIND is a computer code dedicated to emission tomography providing fast simulation of the image formed in the detector. It describes a standard SPECT (*Single Photon Emission Computed Tomography*) camera and can easily be modified for almost any type of calculation or measurement encountered in SPECT imaging. It was used for obtaining detailed and realistic simulations of the auto-radiographies. SIMIND has the advantage of using numerically defined 3-D source and phantoms. For an autoradiography experiment the source coincides with the phantom. For their numerical definition we used the 3-D tomographic reconstruction of the non-irradiated HFTM capsule [1]. Using image segmentation techniques the 3-D model of the capsule was isolated and extracted (Fig. 6). It was used as an input for SIMIND in the form of 256 consecutive images with 256 x 256 pixels.

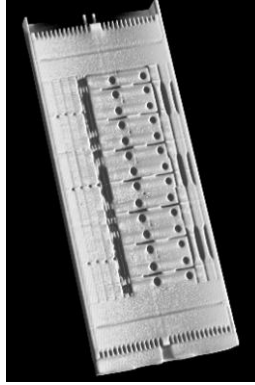


Figure 6 – 3D reconstruction of the HFTM irradiation capsule

The ratio between the energy deposition in the detector produced by X-ray and γ -ray, respectively, must be evaluated in order to calibrate the intensity of the simulated auto-radiographies in respect with the measured radiographies. This can be performed by simulating also the formation of the radiography. SIMIND provides the possibility to obtain images in a simulated transmission experiment, but for a fixed energy of the radiation. As the X-ray emitted in tomographic experiments has a polychromatic spectrum, it means that the spectrum must be discretized and SIMIND must be run for each discrete component of the spectrum. This is, of course, a very time consuming procedure. In order to avoid such extremely inefficient calculations, ITS was used instead of SIMIND. ITS is a general purpose electron/photon transport code, which has the advantage to accommodate the input in energy in the form of a spectrum. However ITS do not accept numerically defined 3-D objects. This is the reason for which the energy deposition induced by the X-ray radiography and by the auto-radiography, respectively, was evaluated for an object with the same volume as the investigated sample, but with cylindrical shape. The cylindrical symmetry also permits the use of *Cyltran*, a version of the ITS code which employs a fully three-dimensional description of particle trajectories within an axisymmetric cylindrical material geometry and which provides much faster calculations than the general transport code. For describing X-ray radiographic image formation an efficient strategy for this simulation is to divide the problem in two steps: 1-D simulation of electron transport and formation of X-ray on the tungsten target and 3-D simulation of photon transport through pre-filters, the object, post-filters to the detector. The simulation of electron transport and formation of X-ray on the tungsten target was performed using *Tiger*, the 1-D multilayer code of ITS package. In the case of γ -ray auto-radiographic image formation, the volume distribution of the gamma activity was modeled by a set of successive circular surfaces, that can be used for source definition in ITS, placed along the cylindrical object.

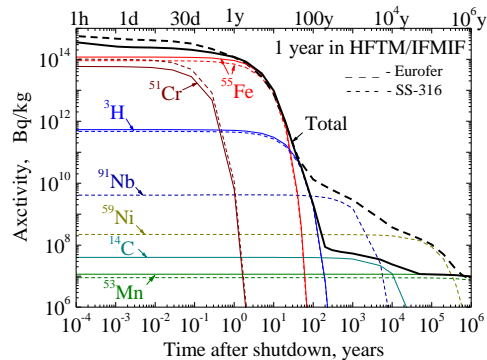


Figure 7 – Total and specific isotope γ -ray activities induced in the Eurofer (solid lines) and SS-316 (dashed lines) steels after 1 year irradiation in the HFTM of the IFMIF.

For a long irradiation time (one up to few years – typical for IFMIF experiments) experimental data concerning the activation of the HFTM irradiation capsule due to neutron activation are not published in the open literature. In our analysis we used the evaluation performed in FZK [6]. Figure 7, obtained by courtesy of Dr. Fischer’s group of FZK, shows that for IFMIF neutron spectrum and intensity, the gamma activity, specific for HFTM case, increases significantly especially due to ^{51}Cr up to specific saturation activity of about 10^{14} Bq/kg. One should note that isotopes as ^{55}Fe , ^3H , ^{14}C do not contribute to the gamma radioactivity.

In our evaluation we determined the energy deposition in the detector for the gamma line of 320 keV of ^{51}Cr after one life time (approximately one month) of cooling period.

Results

Monte-Carlo simulated emission spectra from the transmission tungsten target of the VISCOM X-ray source, irradiated with a 220 keV electron beam is presented in Fig. 8. The total photon flux, normalized to one source electron is $5.405 \cdot 10^{-5}$. A filter of 2.0 mm Cu - was considered in the experiment as a typical active method for beam-hardening artifacts reduction [7]. Fig. 9 presents the corresponding cumulative energy spectrum used as input in the ITS-Cyltran code.

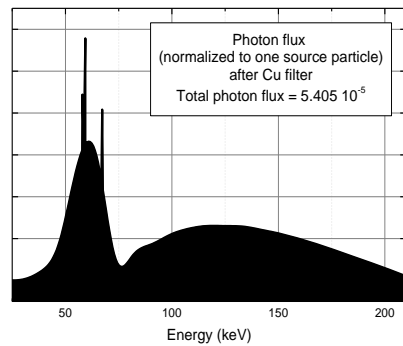


Figure 8 - Energy spectrum of photon flux (after Cu filter)

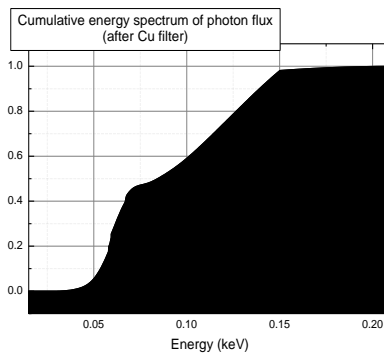


Figure 9 - Cumulative energy spectrum of photon flux (after Cu filter)

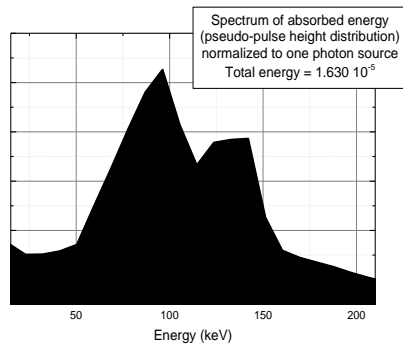


Figure 10 – Pulse height distribution in case of X-ray radiography of HFTM capsule

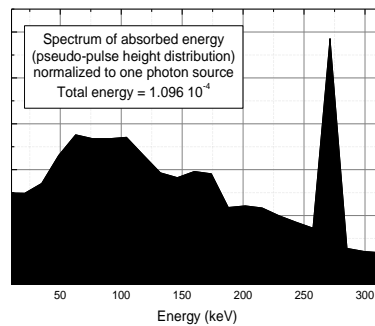


Figure 11 – Pulse height distribution in case of auto-radiography of HFTM capsule

Fig. 10-11 presents the pulse height distribution produced in the detector the by X- and γ -rays, respectively. The total pulse height, corresponding to one source X-ray photon is $1.630 \cdot 10^{-5}$. The total pulse height determined by X-rays, normalized to one electron source is $8.810 \cdot 10^{-10}$. For a X-ray tube current of $650 \mu\text{A}$, the total pulse height becomes $3.597 \cdot 10^6$ counts. In the case of the auto-radiography of the irradiated HFTM capsule, the total pulse height, normalized to one photon source is $1.096 \cdot 10^{-4}$ counts. The gamma activity is significant, especially due to ^{51}Cr . The specific activity after one year irradiation is $\sim 10^{14}$ Bq/kg. Taking into account the mass of the HFTM capsule (~ 700 g) and considering a density of 7.8 g/cm^3 , the total pulse height, becomes $7.670 \cdot 10^9$. Therefore, the ratio between the total pulse height generated by auto-radiography and X-ray radiography is $R_{\gamma\text{-ray}/X\text{-ray}} \cong 2.1 \cdot 10^3$. As expected, in this case, the γ -ray completely perturb the X-ray radiography. The subtraction of the autoradiography from the radiography of the irradiated sample is useless, as revealed by Fig. 12.

In order to reduce this factor one needs to use a collimation system. We evaluated collimators with different slit heights and full width (the width of the collimator covers the entire width of the detector). A schematic illustration is presented in Fig. 13. Using the collimator, radiographic and auto-radiographic data is obtained only for a slice of the investigated object. The measurements must be repeated successively, each time shifting vertically the position of the collimator in order to obtain the data needed to reconstruct the whole object. The value of the vertical shift is equal to the value of the slit height. Therefore it means that the price paid for diminishing the influence of the auto-radiography in the effective image formed on the detector is the increase of number of measurements and of the total time needed to perform the experiment. Taking into account the shape of the collimator it is reasonable to consider the replacement of the 2D matrix detector (typical for cone-beam X-ray tomography) with a linear detector array. The linear detector array provide fast image acquisition and fast data transfer. Therefore it will diminish significantly the total acquisition time.

In the present study we considered a slit height that leads to a value of R close to unity. In this case the influence of the γ -radioactivity of the irradiated HFTM capsule is presented in Fig. 14.

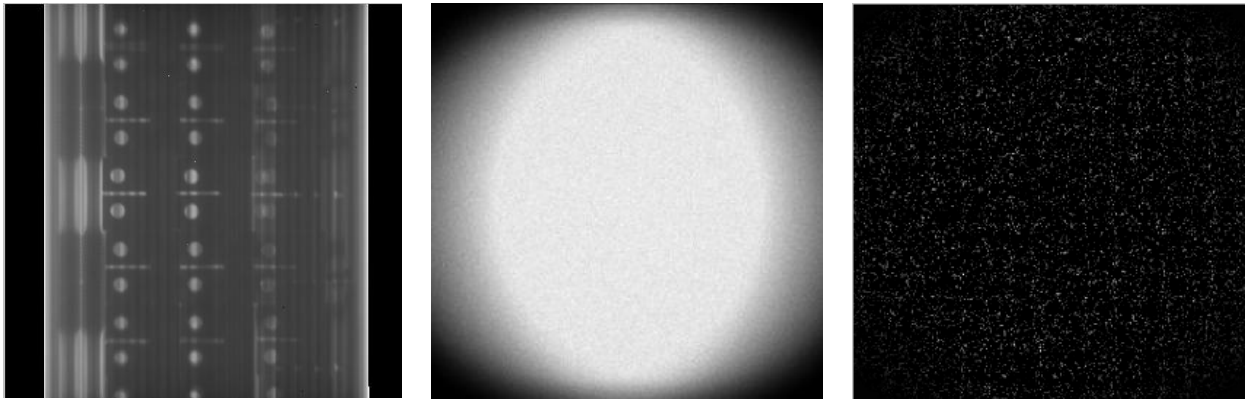


Figure 12 – Influence of the γ -radioactivity of HFTM without using a collimation system: real X-ray radiography I_R (left), - effective image ($I_{eff} = I_R + I_{AR}$) of the irradiated HFTM (middle) and simulated radiography of the irradiated HFTM, after subtraction of the auto-radiograph, $I'_R = I_{eff} - I'_{AR}$ (right)

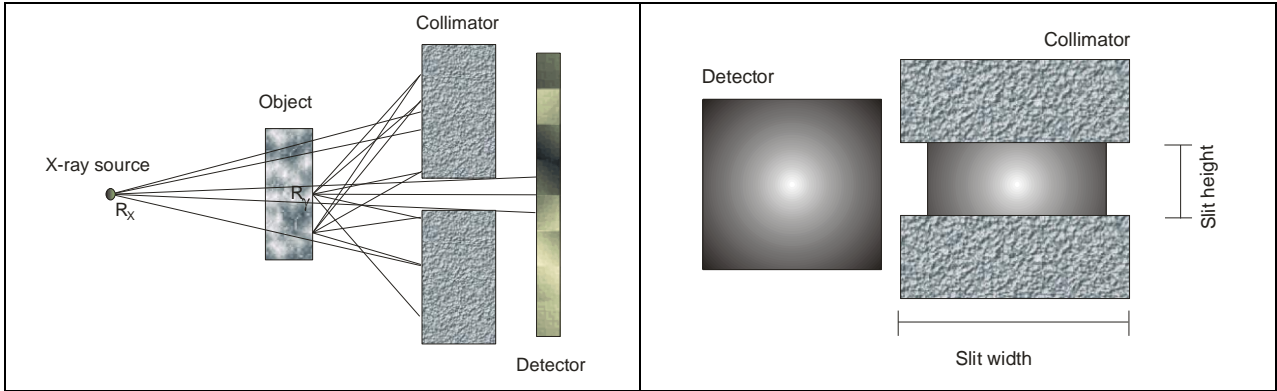


Figure 13 – The collimation system: illustration of the role of the collimator in diminishing the amount of γ -rays in the formed image (left), frontal view illustrating the useful region determined on the detector by the full width collimator (right)

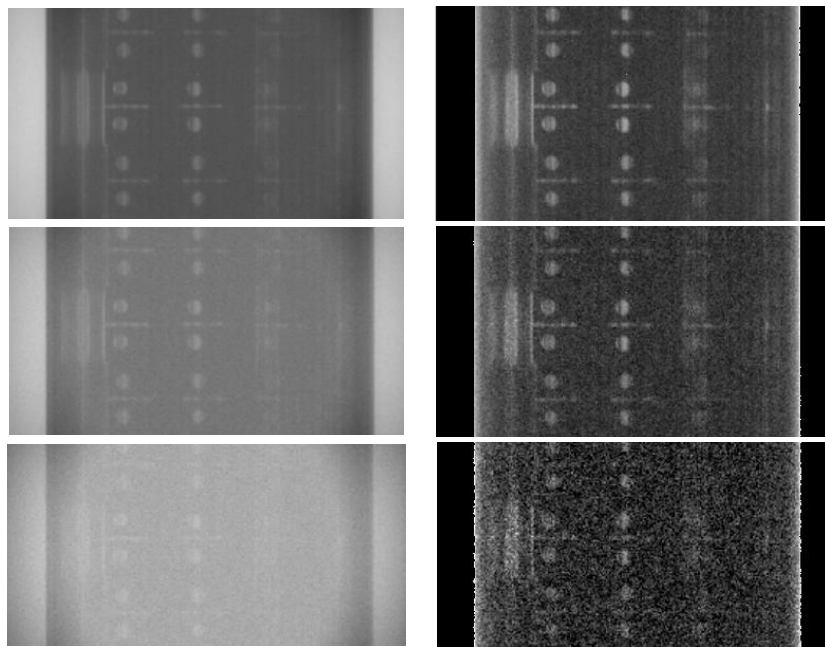


Figure 14 – Influence of the γ -radioactivity of HFTM when using a collimation system with different slit heights: 0.2 mm (top), 0.4 mm (middle) and 1.0 mm (bottom). Effective image $I_{eff} = I_R + I_{AR}$ of the irradiated HFTM (left column) and simulated radiography of the irradiated HFTM after subtraction of the auto-radiography, $I'_R = I_{eff} - I'_{AR}$ (right column)

For a slit width of 0.2 mm the influence of γ -radioactivity is relatively reduced and it consists, after subtraction of the auto-radiography from the X-ray radiography of the irradiated sample, of an additional noise. This level of this noise increases significantly for a slit width of 0.4 mm but almost all of the fine details are still present in the image. For a slit width of 1.0 mm the blurring induced by noise is considerable and only coarse details can be inspected.

Tomographic reconstructions proved to be much more sensitive to the noise induced after subtraction of the autoradiography, as it is illustrated in Fig. 15. For a collimator with a slit height of 0.2 mm shapes are strongly distorted and for a slit height of 0.4 mm the reconstruction is almost meaningless.

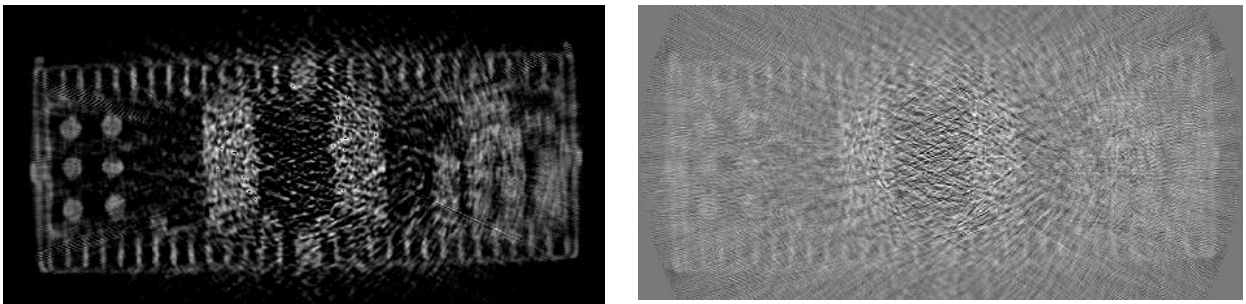


Figure 14 – Axial cross-section through the tomographic reconstruction for a collimator with a slit height of 0.2 mm (left) and 0.4 mm (right).

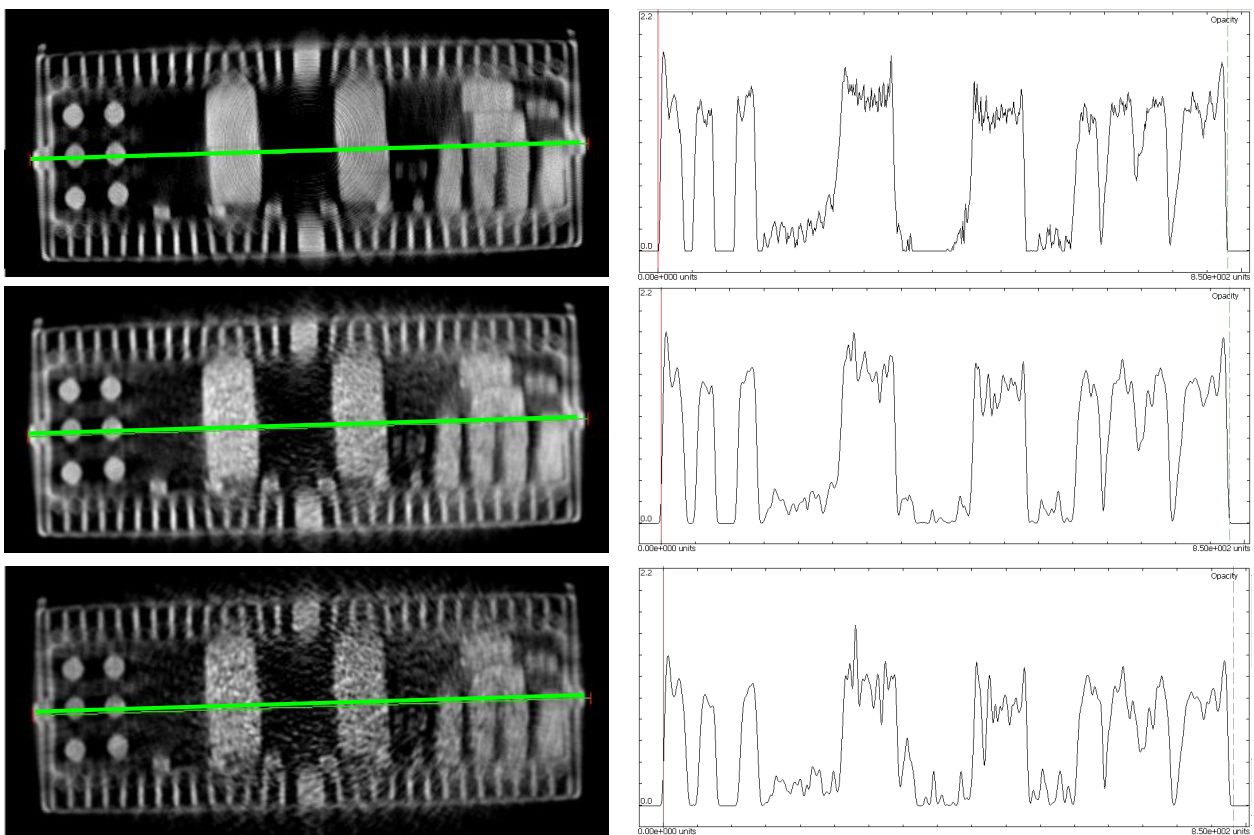


Figure 15 – Axial cross-section through the tomographic reconstruction and line profiles. Top row corresponds to the tomographic reconstruction performed for the non-irradiated HFTM. Middle and bottom rows show the results obtained for the irradiated HFTM when using a collimator with a slit height of 0.05 mm and 0.1 mm respectively.

This result enforces the use of lower value for the slit height in order to get good enough reconstructions, as illustrated in Fig. 15. The quality of the reconstructions can be judged also by comparing the line profiles through the cross section. It is revealed that for both slit height values the peak-shape structure is correctly reproduced and in consequence accurate geometrical measurements can be performed. The accuracy of the shape reconstructions is illustrated in Fig. 16 where the reconstructions are presented after gradient filtering. The price paid for obtaining good reconstructions using lower values for the slit height is, of course, the increase of the time needed to collect the experimental data.

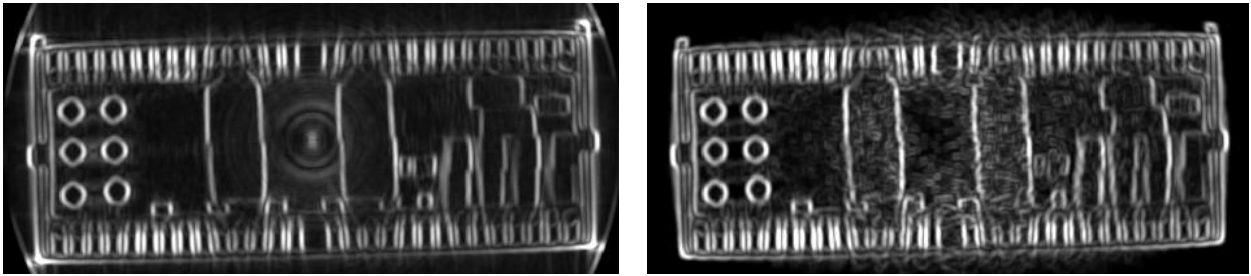


Figure 16 - Axial cross-section through the tomographic reconstruction, after gradient filtering, for the non-irradiated HFTM(left) and for the irradiated HFTM when using using a collimator with a slit height of 0.1 mm.

Conclusion

Extensive tomographic experiments of the full rig were performed and further refinements of the tomographic reconstruction techniques were performed in order to obtain improved quality images. We proved the ability of the tomography inspection to precisely localize and identify the miniaturized samples and the instrumentation elements.

Presently, the X-ray micro-tomography is the only reliable solution for official inspections of the structural integrity of IFMIF complete assemblies before, during maintenance (beam-off) periods and after irradiation campaigns. In consequence evaluation of the influence of the sample radioactivity (produced by neutron activation) on the tomographic reconstruction quality is necessary. The evaluation was performed using real X-ray radiographic data obtained for a non-irradiated HFTM and simulating the gamma radioactivity by Monte Carlo techniques. The numerical simulation working environment was constructed on the basis of two well established Monte Carlo computer codes: SIMIND, which describes SPECT experiments and the integrated TIGER series (ITS) time-independent multimaterial and multidimensional-coupled electron/photon transport code. Latest activation data was incorporated.

The simulations proved, as expected, that the irradiated HFTM can be inspected only by using a collimation system. The optimal parameters of this system were determined. X-ray radiography proved to be more permissive than tomography. However, it is proved that good quality reconstructions can be obtained for a practicable geometry of the collimation system. Shapes are correctly reproduced and accurate geometrical measurements can be performed.

References

1. I. Tiseanu, T. Craciunescu, N.B. Mandache, F. Gherendi - Verification of X-ray microtomography, INTERIM REPORT, EFDA TW5-TTMI-003 D5b, 2005.
2. Tiseanu, M. Simon, T. Craciunescu, B.N. Mandache, V. Heinzl, E. Stratmanns, S.P. Simakov, D. Leichtle - *Assessment of the Structural Integrity of a Prototypical Instrumented IFMIF High Flux Test Module Rig by Fully 3D X-Ray Microtomography*, contribution accepted at the 24th SOFT, under topic: "I -Materials Technology"

3. Ljungberg, M. and Strand, S.-E. - *A Monte Carlo Program Simulating Scintillation Camera Imaging*, *Comp.Meth.Progr.Biomed.* 29, 257-272. 1989.
4. Ljungberg, M., *Simulation Techniques and Phantoms*, in Wernick, M. and Aarsvold, J. *Emission Tomography: The Fundamentals of PET and SPECT*, 2000. Academic Press.
5. J.A. Halbleib, R.P. Kensek, T.A. Mehlhorn, G.D. Valdez, S.M. Seitzer, M.J. Berger, *ITS version 3 – The integrated TIGER series of Coupled Electron/Photon Monte Carlo Transport Codes*, Sandia National Laboratories
6. U. Fischer, S. Simakov, private communication.
7. I. Tiseanu, T. Craciunescu and N.B. Mandache - *Non-destructive analysis of miniaturized samples and irradiation capsules by X-ray micro-tomography*, *Fusion Engineering and Design* Vol 75-79(2005)1005-1059.